CHAPTER 13

Smoke Production and Properties

George W. Mulholland

Introduction

The term *smoke* is defined in this chapter as the smoke aerosol or condensed phase component of the products of combustion. This differs from the American Society for Testing and Materials **(ASTM)** definition of smoke, which includes the evolved gases as well. Smoke aerosols vary widely in appearance and structure, from light colored, for droplets produced during smoldering combustion and fuel pyrolysis, to black, for solid, carbonaceous particulate or soot produced during flaming combustion. A large fraction of the radiant energy emitted from a fire results from the blackbody emission from the soot in the flame. The subject of radiant heat transfer is of such importance that it is treated in a separate chapter. This chapter focuses on smoke aerosols outside the combustion zone.

The effects of the smoke produced by a fire depend on the amount of smoke produced and on the properties of the smoke. The following section presents experimental results on smoke emission for a variety of materials. The smoke emission, together with the flow pattern, determines the smoke concentration as smoke moves throughout a building.

The most basic physical property of smoke is the size distribution of its particles. Results on size distribution for various types of smoke and techniques used for measuring particle size are presented in the section "Size Distribution." The section "Smoke Properties" focuses on those properties of greatest concern to the fire protection community: light extinction coefficient of smoke, visibility through smoke, and detectability of smoke. These properties are primarily determined by the smoke concentration and the particle size distribution. References for other smoke aerosol properties, such as diffusion coefficient and sedimentation velocity, are also provided.

Dr. George W. Mulholland is head of the Smoke Dynamics Research Group in the Center for Fire Research at the National Bureau of Standards. His research has focused on smoke aerosol phenomena and the development of accurate particle size standards.

Smoke Production

Smoke emission is one of the basic elements for characterizing a fire environment. The combustion conditions under which smoke is produced—flaming, pyrolysis, and smoldering—affect the amount and character of the smoke. The smoke emission from a flame represents a balance between growth processes in the fuel-rich portion of the flame and burnout with oxygen. While it is not possible at the present time to predict the smoke emission as a function of fuel chemistry and combustion conditions, it is known that an aromatic polymer, such as polystyrene, produces more smoke than hydrocarbons with single carbon-carbon bonds, such as polypropylene. The smoke produced in flaming combustion tends to have a large content of elemental (graphitic) carbon.

Pyrolysis occurs at a fuel surface as a result of an elevated temperature. This may be due to a radiant flux heating the surface. The temperature of a pyrolyzing sample, 600 to 900 K, is much less than the gas phase flame temperature, 1200 to 1700 K. The vapor evolving from the surface may include fuel monomer, partially oxidized products, and polymer chains. As the vapor rises, the low vapor pressure constituents can condense, forming smoke droplets appearing as light-colored smoke.

Smoldering combustion also produces smoke droplets, but in this case the combustion is self-sustaining, whereas pyrolysis requires an external heat source. While most materials can be pyrolyzed, only a few materials, including cellulosic materials (wood, paper, cardboard, etc.) and flexible polyurethane foam, are able to smolder. The temperature during smoldering is typically 600 to 1100 K.

In Table 2-13.1 the smoke conversion factor, E, is given for a variety of materials commonly found in build-

Table 2-13.1 ***Smoke Production for Wood and Plastics***

Type	Smoke Conversion Factor, E	Combustion Conditions	Fuel Area, m^2	Reference
Douglas fir	0.03-0.17	Pyrolysis	0.005	1
Douglas fir	< 0.01-0.025	Flaming	0.005	1
Hardboard	0.0004-0.001	Flaming[a]	0.0005	2
Fiberboard	0.005–0.01	Flaming[a]	0.0005	2
Polyvinylchloride	0.03–0.12	Pyrolysis	0.005	3
Polyvinylchloride	0.12	Flaming	0.005	1
Polyurethane (flexible)	0.07–0.15	Pyrolysis	0.005	3
Polyurethane (flexible)	< 0.01-0.035	Flaming	0.005	1
Polyurethane (rigid)	0.06–0.19	Pyrolysis	0.005	1
Polyurethane (rigid)	0.09	Flaming	0.005	1
Polystyrene	0.17 (m_{O_2} = 0.30)[b]	Flaming	0.0005	4
Polystyrene	0.15 (m_{O_2} = 0.23)	Flaming	0.07	5
Polypropylene	0.12	Pyrolysis	0.005	1
Polypropylene	0.016	Flaming	0.005	1
Polypropylene	0.08 (m_{O_2} = 0.23)	Flaming	0.007	5
Polypropylene	0.10 (m_{O_2} = 0.23)	Flaming	0.07	5
Polymethylmethacrylate	0.02 (m_{O_2} = 0.23)	Flaming	0.07	5
Polyoxymethylene	- 0	Flaming	0.007	5
Cellulosic insulation	0.01-0.12	Smoldering	0.02	6

[a]Sample smoldered for a period of time alter the pilot flame was extinguished.
[b]m_{O_2} refers to mol fraction of O

ings. The quantity E is defined as the mass of smoke produced/mass of fuel burned.

The references cited in Table 2-13.1 should be consulted regarding the detailed description of the combustion conditions. In many instances,[1,3] E was measured for a range of radiant fluxes, oxygen concentrations, sample orientations, and ambient temperatures. It is seen in Table 2-13.1 that E has a greater range for flaming combustion, with values in the range 0.001 to 0.17, compared to pyrolysis and smoldering, with values in the range 0.01 to 0.17. The following factors should be taken into account when using this table for smoke emission estimates:

1. Most of the measurements reported in Table 2-13.1 were made on small-scale samples.
2. Most experiments were for free burning at ambient conditions; reduced ventilation can strongly affect the smoke production.
3. In transport, the smoke may coagulate, partially evaporate, and deposit on surfaces through diffusion and sedimentation. **Also,** additional smoke may be formed through condensation.

Size Distribution

Smoke particle size distribution, together with the amount of smoke produced, primarily determines the properties of the smoke. **A** widely used representation of the size distribution is the geometric number distribution, $\Delta N/\Delta \log d$, versus $\log d$, where d represents the particle diameter. The quantity **AN** represents the number of particles per cm3, with diameter between logd and logd $+\Delta \log d$. **As** an example, the particle size distribution of

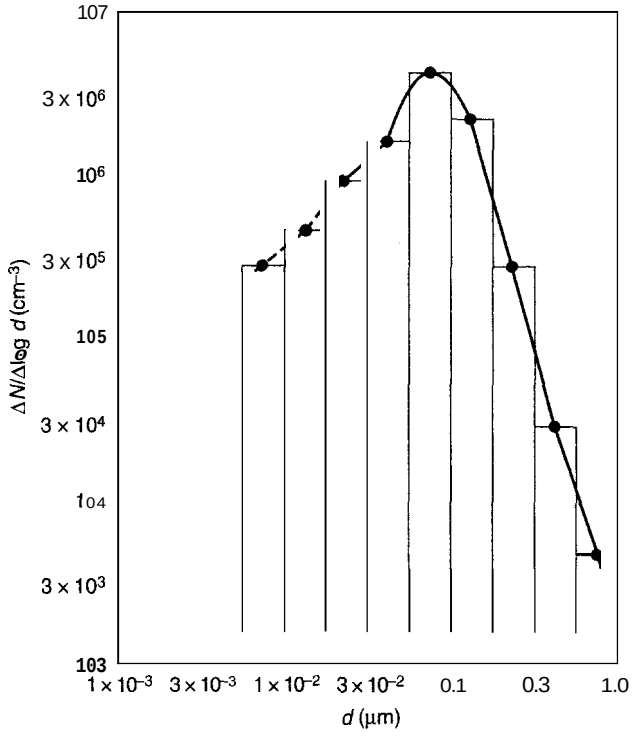

Figure 2-13.1. ***Size distribution of incense smoke as measured by an electrical aerosol analyzer. There is a large uncertainty in the dashed portion of the curve.***

smoke produced by a smoldering incense stick is plotted in Figure 2-13.1, where Alog d for each discrete size range equals 0.25. In this case, the total number concentration for a given size range equals $0.25(\Delta N/\Delta \log d)$. It is seen that the logarithmic scale is necessitated by the wide range in particle size and concentration.

For many applications, the most important characteristics of a size distribution are the average particle size and the width of the distribution. A widely used measure of the average size is the geometric mean number diameter, d_{gn}, defined by

$$\log d_{gn} = \sum_{i=1}^{n} \frac{N_i \log d_i}{N} \tag{1}$$

where

N = total number concentration

N_i = number concentration in the ith interval

log is to the base 10

For the size distribution plotted in Figure 2-13.1, $d_{gn} = 0.072\ \mu\text{m}$.

The corresponding measure of the width of the size distribution is the geometric standard deviation, σ_g,

$$\log \sigma_g = \left[\sum_{i=1}^{n} \frac{(\log d_i - \log d_{gn})^2 N_i}{N} \right]^{1/2} \tag{2}$$

For the size distribution plotted in Figure 2-13.1, $\sigma_g = 1.75$. A perfectly monodisperse distribution would correspond to $\sigma_g = 1$. The parameters d_{gn} and σ_g are useful because actual size distributions are observed to be approximately log-normal, which is the same as a normal or Gaussian distribution, except that log d is normally distributed instead of d. An important characteristic of the log-normal distribution is that 68.3 percent of the total particles are in the size range $\log d_{gn} \pm \log \sigma_g$; for $d_{gn} = 0.072\ \mu\text{m}$ and $\sigma_g = 1.75$, this corresponds to the size range of 0.041 to 0.126 μm.

EXAMPLE 1:

Compute d_{gn} and σ_g for the data given below:

Interval, μm	d_i	N_i, cm^{-3}	log d_i	$N_i \times \log d_i$, cm^{-3}
0.0056-0.01	0.0078	6×10^4	−2.11	-1.27×10^5
0.010-0.018	0.014	2 x 105	−1.85	−3.7 x 105
0.018-0.032	0.025	4 x 105	−1.60	−6.40 x 105
0.032–0.056	0.044	9 x 104	−1.36	−1.22 x 105
0.056-0.10	0.078	3 x 104	−1.11	−3.33 x 104
0.10–0.18	0.14	1 x 103	−0.85	−0.85 x 103
		7.81 x 105		-1.30×10^6

SOLUTION:

$$d_{gn} = 10^{(-1.30\times10^6/7.81\times10^5)} = 0.022\ \mu\text{m}$$

Compute the geometric standard deviation:

N_i	log d_i	log d_i − log d_{gn}	N_i(log d_i − log d_{gn})^2
6 × 104	−2.11	−0.45	1.22 x 104
2 × 105	−1.85	−0.19	7.2 x 103
4×10^5	−1.60	0.06	1.4 x 103
9 x 104	−1.36	0.30	8.1 x 103
3 x 104	−1.11	0.55	9.1 x 103
1 x 103	−0.85	0.81	6.5×10^2
7.81 x 105			3.87 x 104

SOLUTION:

$$\sigma_g = 10^{(3.87\times10^4/7.81\times10^5)^{0.5}} = 1.67$$

The size distribution plotted in Figure 2-13.1 is based on electrical mobility analysis of the smoke aerosol. Figures 2-13.2 and 2-13.3 show size distributions of droplet smoke produced by smoldering cellulosic insulation, as measured by an optical particle counter and by two cas-

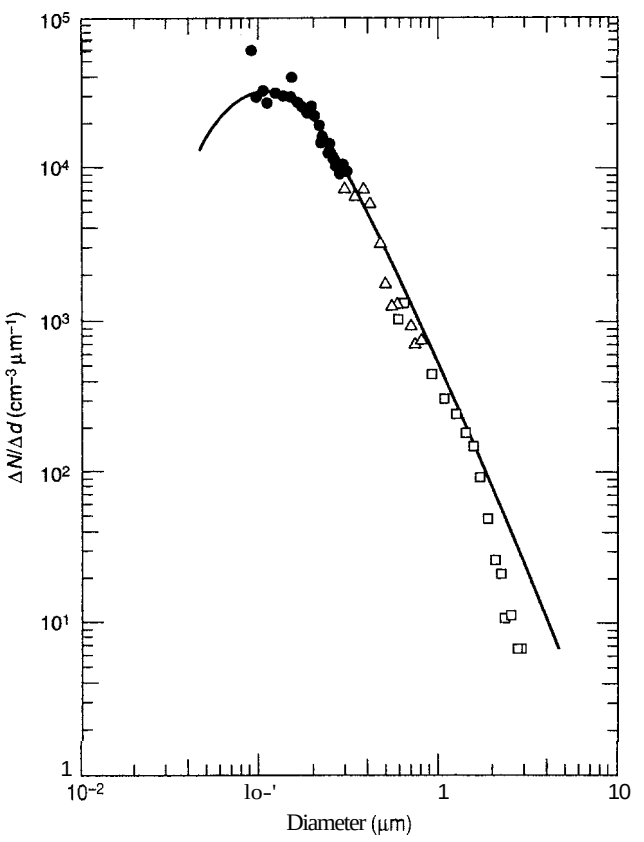

Figure 2-13.2. ***The number size distribution of smoke generated by smoldering cellulosic insulation as measured by an optical particle counter. The symbols correspond to the particle size range settings of the instrument, and the smooth curve is an exponentially truncated power law distribution fit to the data.***

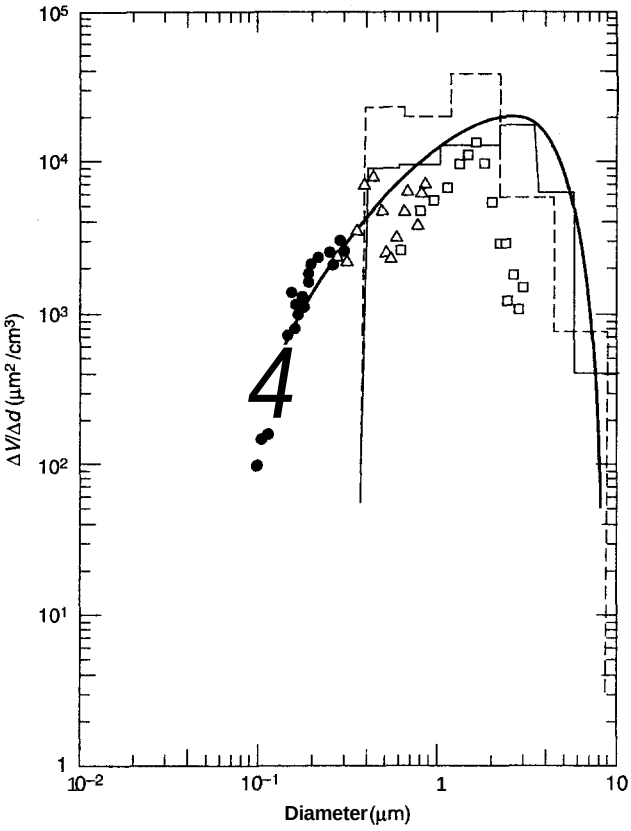

Figure 2-13.3. ***The volume size distribution of smoke obtained from the optical particle counter, quartz crystal microbalance cascade impactor (dashed histogram), and Andersen impactor (solid histogram). The smooth curve represents the exponentially truncated power law distribution.***

cade impactors.6 The smoke volume distribution plotted in Figure 2-13.3 for the optical particle counter is obtained from the number distribution, using the following relation:

$$V_i = N_i \frac{1}{6} \pi d_i^3 \tag{3}$$

For particles sized above 1 pm, impactors provide more reliable information on the smoke volume distribution than optical particle counters. An optical particle counter is the preferred instrument for the number distribution measurement.

To correlate the smoke volume/ particle size distribution, the geometric mean volume diameter, d_{gv}, is a convenient measure of average particle size:

$$\log d_{gv} = \frac{\sum_{i=1}^{n} V_i \log d_i}{V_T} \tag{4}$$

where V_T is the total volume concentration of the smoke aerosol. For a log-normal distribution, there is the following relationship between the geometric mean volume diameter, d_{gv}, and the geometric mean number diameter, d_{gn}:

$$\log d_{gv} = \log d_{gn} + 6.9(\log \sigma_g)^2 \tag{5}$$

In the case of smolder smoke, σ_g is above 2.4. This large value of σ_g results in a large difference between d_{gn} and d_{gv}, 0.2 µm versus 2 pm, respectively. Some devices, such as an ionization-type smoke detector, have an output depending primarily on d_{gn}, while others, such as light-scattering-type detectors, have an output depending more on d_{gv}. More than one instrument is necessary for a complete characterization of the smoke size distribution, because it is typically quite wide.

A list of commercially available instruments for measuring smoke aerosol concentration and particle size distribution is given in Table 2-13.2. Smoke measurements pose special problems because of the high concentration, wide particle size range, and sometimes high temperature. In selecting an instrument it is important to make the following considerations:

1. Will the instrument respond to the smoke of interest? For example, the piezoelectric mass monitor does not respond well to soot.
2. Will dilution of the smoke be required?
3. Is the measurement size range of the instrument adequate?
4. Is a mass or number distribution measurement appropriate?
5. What is the particle size resolution needed?
6. Is real-time measurement capability needed?
7. Will the instrument perform at the temperature of the smoke environment?

In Table 2-13.3, average particle size and the width of the size distribution are presented for smoke generated by a variety of materials. The results are most meaningful for smoke droplets produced during pyrolyzing and smoldering combustion. In the case of flaming combustion, complex soot agglomerates are formed as shown in Figure 2-13.4. For soot agglomerates, unlike for spherical smoke droplets, the apparent particle size depends on the measurement technique.

Smoke aerosols are dynamic with respect to their particle size distribution function. Smoke particles or droplets undergoing Brownian motion collide and stick together. The result of this behavior is that, in a fixed volume of smoke-laden gas, the number of particles decreases while the total mass of the aerosol remains unchanged. This process is known as coagulation. The fundamental parameter for describing coagulation is the coagulation coefficient, Γ, the rate constant for the coagulation equation

$$\frac{dN}{dt} = -\Gamma N^2 \tag{6}$$

Γ was found to be about 4×10^{-10} cm³/s for smoke produced from incense sticks and about 1×10^{-9} cm³/s for

Table 2-13.2 ***Operational Characteristics of Commercially Available Instruments for Smoke Characterization***

Instrument Type	Function/Range	Advantage/Limitation for Smoke Measurements
Filter-collection	Mass conc.	Accurate, slow
Piezoelectric mass monitor	Mass conc. $0.01 < d < 5$ μm	Real-time output, but dilution required if >20 mg/m³; does not respond well to soot
Tapered element oscillating microbalance	Mass conc. <5 μm	Real time, 0.1–1000 mg/m³; replace filter after 3–100 mg deposit
Condensation nuclei counter	Number conc. $0.005 < d < 2$ μm	<3 × 105 particles/cm³
Photometer	Scattered light 0.1–10 μm	1.1–1000 mg/m³
Nephelometer	Total light scattered	<5 mg/m³
Electrical aerosol analyzer	Size distribution $0.01 < d < 0.3$ μm	<5 × 10⁵ particles/cm³; 2 min/scan
Cascade impactor	Mass size distribution[a] $0.5 < d < 10$ μm	No dilution needed, can be used at high temp., large sample required
Optical particle counter	Number distribution[b] $0.5 < d < 10$ μm	Highest resolution, <10³ particles/cm³, large dilution

[a]Low-pressure impactor extends size range down to 0.05 μm.
[b]Laser model extends size range down to 0.1 μm and concentration up to 10⁴ particles/cm³.

smoke produced from flaming α-cellulose.[7] The coagulation process has a more pronounced effect on the number distribution than the mass distribution as small particles collide to form larger particles.

EXAMPLE 2:

Calculate the change in the number concentration over a 5-min time interval for a uniformly distributed smoke, generated from flaming a-cellulose given an initial concentration of 1×10^7 particles/cm³.

Integrating Equation 6 yields

$$N = \frac{N_0}{1 + \Gamma N_0 t} = \frac{1 \times 107}{1 + (10^{-9})(10^7)(300)} = \frac{107}{1+3}$$

$$N = 2.5 \times 10^6 \text{ particles/cm}^3$$

So in this example, there is a fourfold reduction in number concentration due to coagulation.

The effect of the decrease in number concentration on the size distribution is treated by Mulholland et al.[25] A

Table 2-13.3 ***Particle Size of Smoke from Burning Wood and Plastics***

Type	d_{gm}, μm[a]	d_{32}, μm[b]	σ_g	Combustion Conditions	Reference
Douglas fir	0.5–0.9	0.75–0.8	2.0	Pyrolysis	1, 3
Douglas fir	0.43	0.47–0.52	2.4	Flaming	1, 3
Polyvinylchloride	0.9–1.4	0.8–1.1	1.8	Pyrolysis	3
Polyvinylchloride	0.4	0.3–0.6	2.2	Flaming	3
Polyurethane (flexible)	0.8–1.8	0.8–1.0	1.8	Pyrolysis	3
Polyurethane (flexible)		0.5–0.7		Flaming	3
Polyurethane (rigid)	0.3–1.2	1.0	2.3	Pyrolysis	3
Polyurethane (rigid)	0.5	0.6	1.9	Flaming	3
Polystyrene		1.4		Pyrolysis	1
Polystyrene		1.3		Flaming	1
Polypropylene		1.6	1.9	Pyrolysis	1
Polypropylene		1.2	1.9	Flaming	1
Polymethylmethacrylate		0.6		Pyrolysis	1
Polymethylmethacrylate		1.2		Flaming	1
Cellulosic insulation	2–3		2.4	Smoldering	6

[a]d_{gm} is analogous to d_{gv}, but with mass replacing volume in Equation 4. Values of d_{gm} less than about 0.5 μm are probably overestimates arising from the minimum size resolution of the impactor at about 0.4 μm.
[b]The quantity d_{32} is obtained by optical measurements

$$d_{32} = \frac{\sum_{i=1}^{n} N_i d_i^3}{\sum_{i=1}^{n} N_i d_i^2}$$

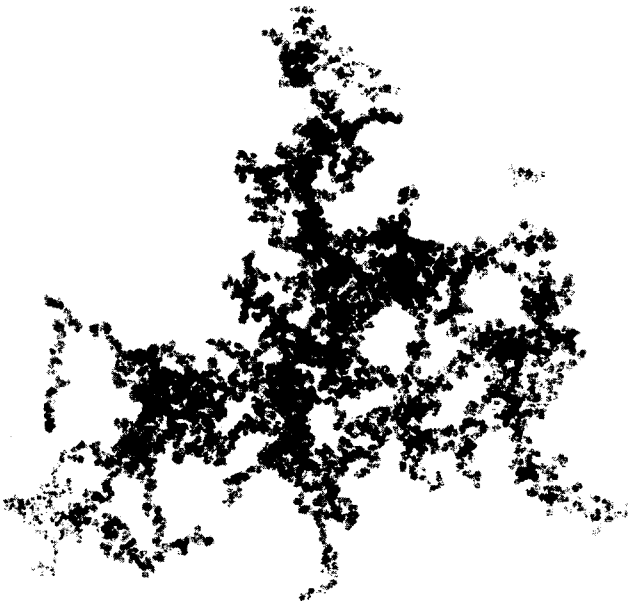

Figure 2-13.4. ***Transmission electron micrograph of a soot particle. The overall size of the agglomerate is about 6 pm, and the diameter of the individual spherules is about 0.03 μm.***

general discussion of coagulation phenomena in aerosols is given by Friedlander.[8] In addition to coagulation, other smoke-aging processes, including condensation of vapor onto existing particles and evaporation of the volatile component of the smoke, can also take place. There is relatively little information on these processes. Also, smoke particles can be lost to the walls, ceiling, and floor of an enclosure through a variety of processes, including diffusion, sedimentation, and thermophoresis.

Smoke Properties

The smoke properties of primary interest to the fire community are light extinction, visibility, and detection. For completeness, a list of other smoke aerosol properties and references is given in Table 2-13.4.

Table 2-13.4 ***Smoke Aerosol Properties***

Property	Reference
Diffusion coefficient	8
Sedimentation velocity	9
Thermophoretic velocity	10
Aerodynamic diameter	9
Electrical mobility	9
Thermal charging	9
Scattering coefficient	8
Extinction coefficient	8
Condensation/evaporation	8

The most widely measured smoke property is the light extinction coefficient. The physical basis for light extinction measurements is Bouguer's law, which relates the intensity, I_0^λ, of the incident monochromatic light of wavelength λ and the intensity of the light, I_λ, transmitted through the pathlength, L, of the smoke:

$$\frac{I_\lambda}{I_\lambda^0} = e^{-KL} \tag{7}$$

where K is the light extinction coefficient. When Equation 7 is expressed in terms of base 10,

$$\frac{I_\lambda}{I_\lambda^0} = 10^{-DL} \tag{8}$$

The quantity D is defined as the optical density per meter, and $D = K/2.3$.

The extinction coefficient, K, is an extensive property and can be expressed as the product of an extinction coefficient per unit mass, K_m, and mass concentration of the smoke aerosol, m.

$$K = K_m m \tag{9}$$

The specific extinction coefficient, K_m, depends on the size distribution and optical properties of the smoke through the relation

$$K_m = \frac{3}{2\rho m}\int_{d_{\min}}^{d_{\max}} \frac{1}{d}\frac{\Delta m}{\Delta d} Q_{\text{ext}}\left(\frac{d}{\lambda}, n_r\right) \delta d \tag{10}$$

In Equation 10 the symbol $\Delta m/\Delta d$ represents the mass size distribution. The single particle extinction efficiency, Q_{ext}, is a function of the ratio of particle diameter to wavelength of light, d/λ, and of the complex refractive index of the particle, n_r.[8] The quantity ρ represents the particle density.

Seader and Einhorn[11] obtained K_m values of 7.6 m^2/g for smoke produced during flaming combustion of wood and plastics and a value of 4.4 m^2/g for smoke produced during pyrolysis of these materials. The experiments were small scale, utilizing samples of about 50 cm^2, and the value of K_m represents an integrated result for the entirety of the test. The light source used in the measurements was polychromatic, while Bouguer's law is strictly valid only for monochromatic light. Foster[12] predicted a 22 percent deviation from Bouguer's law over the mass concentration range from 0.06 to 2.8 g/m^3 as a result of using a polychromatic light source with wood smoke. Still, it is useful to use the Seader and Einhorn[11] result as a rough guide if more detailed optical data on the smoke of interest is not available.

Mulholland[13] has described the general design of a light extinction instrument that satisfies Bouguer's law. Two key features are the use of monochromatic light and the elimination of forward scattered light at the detector.

The specific optical density, D_s, is measured in a standard laboratory smoke test[14] for assessing the amount of visible smoke produced in a fire. The dimensionless quantity D_s is defined by

$$D_s = \frac{DV_c}{A} \tag{11}$$

where V_c is the volume of the chamber, and A is the area of the sample. D_s is a convenient quantity to measure if the decomposed area is well defined. Since D_s depends on the sample thickness, the same thickness should be used for relative rating of materials tested. Table 2-13.5 includes results for D_s based on small-scale experiments with wood and plastics by Gross et al.,[14] Seader and Chien,[15] and Breden and Meisters.[16] Lopez[17] demonstrated a correlation for D_s between small- and large-scale fires with aircraft interior construction materials.

Table 2-13.5 ***Specific Optical Density and Mass Optical Density for Wood and Plastics***

Type (Sample #)	Maximum D_s	D_m (m²/g)[a]	Combustion Conditions	Sample[b] Thickness (cm)	Reference
Hardboard	6.7×10^1		Flaming	0.6	14
Hardboard	6.0×10^2		Pyrolysis	0.6	14
Plywood	1.1×10^2		Flaming	0.6	14
Plywood	2.9×10^2		Pyrolysis	0.6	14
Polystyrene	$>6.6 \times 10^2$		Flaming	0.6	14
Polystyrene	3.7×10^2		Pyrolysis	0.6	14
Polyvinylchloride	$>6.6 \times 10^2$		Flaming	0.6	14
Polyvinylchloride	3.0×10^2		Pyrolysis	0.6	14
Polyurethane foam	2.0×10^1		Flaming	1.3	14
Polyurethane foam	1.6×10^1		Pyrolysis	1.3	14
Nylon carpet	2.7×10^2		Flaming	0.8	14
Nylon carpet	3.2×10^2		Pyrolysis	0.8	14
Acrylic	1.1×10^2		Flaming	0.6	14
Acrylic	1.6×10^2		Pyrolysis	0.6	14
Plywood	5.3×10^2	0.29	Pyrolysis	0.6	15
Polymethylmethacrylate	7.2×10^2	0.15	Pyrolysis	0.6	15
Polyvinylchloride	1.8×10^2	0.12	Pyrolysis	0.6	15
Polyvinylchloride (with plasticizer)	3.5×10^2	0.64	Pyrolysis	0.6	15
Neoprene	8.8×10^2	0.55	Pyrolysis	0.6	15
Douglas fir	6.2×10^2	0.28	Pyrolysis	0.6	15
Polypropylene	4.0×10^2	0.53	Flaming[c]	0.4	16
Polyethylene	2.9×10^2	0.29	Flaming[c]	0.4	16
Paraffin wax	2.3×10^2	0.23	Flaming[c]	0.4	16
Polystyrene		1.4	Flaming[c]	0.4	16
Styrene		0.96	Flaming[c]	0.4	16
Polyvinylchloride		0.34	Flaming[c]	0.4	16
Polyoxymethylene		-0	Flaming[c]	0.4	16
Polyurethane (7A)	2.1×10^2		Flaming	1.3	17
Polyurethane (7A)	1.5×10^2		Flaming[d]	1.3	17
Wool (8A)	$>5.5 \times 10^2$		Flaming	0.9	17
Wool (8A)	2.2×10^2		Flaming[d]	0.9	17
Acrylic (9B)	5.8×10^1		Flaming	0.14	17
Acrylic (9B)	1.2×10^2		Flaming[d]	0.14	17
Polyurethane (MO1)		0.33	Flaming[c]		18
Polyurethane (MO1)		0.22	Flaming[e]		18
Cotton (MO3)		0.17	Flaming[c]		18
Cotton (MO3)		0.12	Flaming[e]		18
Latex (MO4)		0.65	Flaming[c]		18
Latex (MO4)		0.44	Flaming[e]		18
Neoprene (MO8)		0.40	Flaming[c]		18
Neoprene (MO8)		0.20	Flaming[e]		18
Polystyrene (7)		0.79	Flaming[c]		19
Polystyrene (7)		1.0	Flaming[f]		19
Polystyrene foam (16)		0.79	Flaming[c]		19
Polystyrene foam (16)		0.82	Flamingf		19
ABS (18)		0.52	Flaming[c]		19
ABS (18)		0.54	Flaming[f]		19

[a]The value of D_m is computed by Quintiere,[20] based on data in Babrauskas.18
[b]Sample area is 0.005 m² in vertical configuration, unless stated otherwise.
[c]Sample is in horizontal configuration (0.005 m²).
[d]0.09 m² sample size.
[e]The sample is a mattress.
The sample is a plastic utility table.

If the mass loss of the sample is measured, then the mass optical density, D, is the appropriate measure of visible smoke.

$$D_m = \frac{DV_c}{\Delta M} \tag{12}$$

This technique requires an accurate measurement of the mass loss of the sample, ΔM, in addition to a light extinction measurement. Table 2-13.5 includes results for D_m for a variety of materials studied by Seader and Chien,[15] Breden and Meisters,[16] Babrauskas,[18] and Evans.[19] The results of Babrauskas' study were expressed in terms of D_m by Quintiere.[20]

In two of the studies,[18,19] a comparison was made between D_m measured in small-scale tests and D_m measured in large-scale tests. The large-scale tests involved mattresses[18] in one case and plastic utility tables19 in the other. In these two cases, there appeared to be a qualitative correlation between D_m measured for small- and large-scale tests. Quintiere[20] has made an extensive investigation of the correlation between small- and large-scale studies in terms of D_m and D_s and finds that the correlation breaks down as fires become more complex. From his review of the literature, Quintiere[20] suggests that heat flux and ventilation conditions can have a major effect on smoke production.

In most cases of practical interest, an important goal is to be able to predict the extinction coefficient based on information regarding D_s or D_m. The extinction coefficient, in turn, is related to visibility through the smoke, as discussed below.

Visibility

Visibility of exit signs, doors, and windows can be of great importance to an individual attempting to survive a fire. To see an object requires a certain level of contrast between the object and its background. For an isolated object surrounded by a uniform, extended background, contrast, C, can be defined as[21]

$$C = \frac{B}{B_0} - 1 \tag{13}$$

where B is the brightness or luminance of the object, and B_0 is the luminance of the background. For daylight conditions, with a black object being viewed against a white background, a value of $C = -0.02$ is often used as the contrast threshold at which an object can be discerned against the background. The visibility of the object, S, is the distance at which the contrast is reduced to -0.02. Most visibility measurements through smoke have relied on test subjects to determine the distance at which the object was no longer visible rather than the actual measurement of C with a photometer.

Visibility depends on many factors, including the scattering and the absorption coefficient of the smoke, the illumination in the room, whether the sign is light emitting or light reflecting, and the wavelength of the light. Visibility also depends on the individual's visual acuity and on whether the eyes are "dark-" or "light-adapted." Nevertheless, a fair correlation between visibility of test subjects and the extinction coefficient of the smoke has been obtained in an extensive study by Jin[22] as illustrated in Figure 2-13.5. The visibility of light-emitting signs was found to be two to four times greater than light-reflecting signs. The following expressions were found to correlate the data:

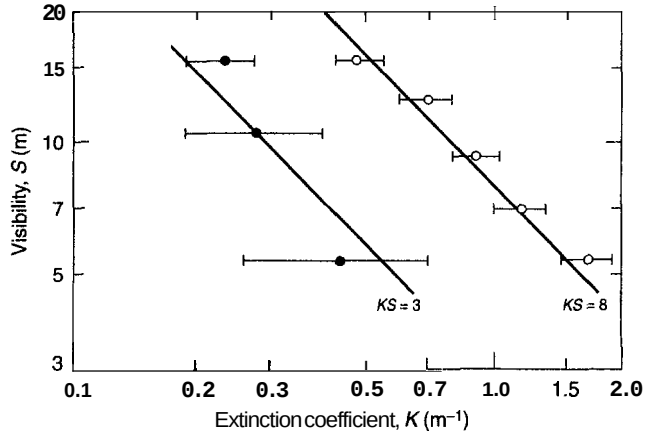

Figure 2-13.5. ***Visibility versus extinction coefficient for a light-emitting sign (O) and light-reflecting sign (●). The range bars include data for both flame- and smolder-generated smoke and sign illumination levels varying by about a factor of 4.***

$$KS = 8 \quad \text{light–emitting sign} \tag{14}$$

$$KS = 3 \quad \text{light-reflecting sign} \tag{15}$$

The data is based on subjects viewing smoke through glass so that the irritant effect of the smoke was eliminated. Jin and Yamada[23] have studied the visual acuity and eyeblink rate for highly irritant white smoke produced by burning wood cribs. They found that the ratio of visual acuity without goggles to acuity with goggles decreases markedly for smoke extinction coefficient, K, greater than $0.25\ \text{m}^{-1}$.

EXAMPLE 3:

Estimate the visibility of a light-reflecting exit sign in a 6-m square room with a 2.5-m height, as a result of flaming combustion of a 200-g polyurethane foam pillow.

The smoke yield for flexible polyurethane, according to Table 2-13.1, is about 0.03 for flaming combustion. This implies a smoke emission, M_s, given by

$$M_s = (0.03)(200) = 6\ \text{g}$$

The corresponding mass concentration in the room, m, is

$$m = \frac{6}{(6)^2(2.5)} = 0.067\ \text{g/m}^3$$

Taking K_m to be $7.6\ \text{m}^2/\text{g}$ for flaming combustion, one obtains K using Equation 9,

$$K = (7.6)(0.067) = 0.51\ \text{m}^{-1}$$

The visibility is next estimated using Equation 15,

$$S = \frac{3}{K} = \frac{3}{0.51} = 5.9 \text{ m}$$

It is important to point out the approximations made in this analysis.

1. The smoke is confined to the room and is well mixed. Actually the concentration will be higher near the ceiling and decrease abruptly below the flame.
2. The value of 0.03 for the smoke conversion factor, ε, is an estimated value in the upper part of the range (0.01 to 0.035) for generic flexible polyurethane foams measured in small-scale experiments and may not be appropriate for a pillow. In a realistic case, the pillow would probably smolder before flaming, and ε is much larger in the smolder mode.
3. The value of K_m is based on a limited number of small-scale experiments with a polychromatic light source.
4. The range of validity of Equation 15 has not been widely studied.

An alternative method for estimating the visibility is based on using the mass optical density data in Table 2-13.5. The quantity D_m for the pillow is estimated to be 0.22 m^2/g based on Babrauskas' results[18] given in Table 2-13.5 for polyurethane (MO1). On rearranging Equation 12, the following result is obtained:

$$D = \frac{D_m \Delta M}{V_c} = \frac{(0.22)(200)}{(6)^2(2.5)} = 0.49 \text{ m}^{-1}$$

The smoke extinction coefficient, K, is $1.12 m^{-1}$ or 2.3 times D. Using Equation 15, we obtain S = 2.7 m compared to 5.9 m obtained by the first method. In principle, the second method is more reliable, because it is more direct.

Detection

In addition to their utility for estimating visibility, light extinction measurements are also widely used in characterizing smoke detector performance. Underwriters Laboratories' (UL) acceptance testing of smoke detectors24 is based in part on a minimum sensitivity based on optical density per meter, D, of 0.06 (4 percent obscuration per ft for a 5 ft beam length) for gray (cellulosic) smoke and 0.14 (10 percent per ft) for black smoke (kerosene).

The electrical output of a detector, P, from a light-scattering or ionization-type smoke detector can be represented as an integrated product of the size distribution function and the basic response of the detector, $R(d)$.

$$P = \int_{d_{min}}^{d_{max}} R(d) \frac{\delta N}{\delta d} \delta d \qquad (16)$$

The response functions for two smoke detectors are plotted in Figure 2-13.6. It is seen that the ionization-type smoke detector is more sensitive to smoke particles smaller than about 0.3 μm, and the light-scattering type more sensitive to particles larger than 0.3 pm.

The basic principle of ionization detectors is the interception of gaseous ions by smoke particles, reducing the ion current in the detector until a preset alarm point is reached. The detector response function is approximately proportional to the product of the number concentration and particle diameter.[25,26] For one detector[25] the response function is given by

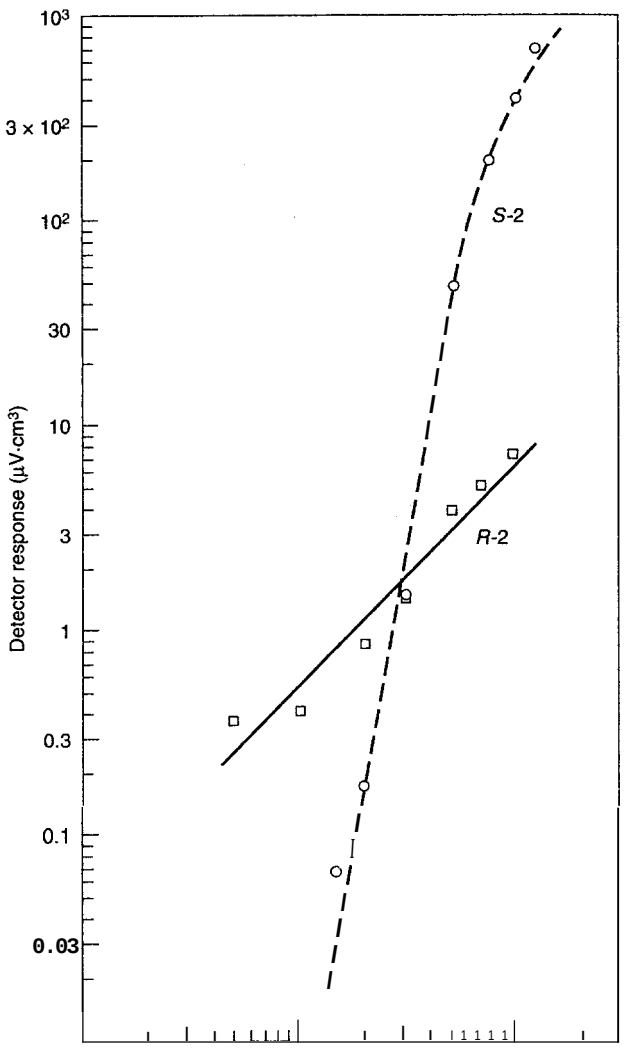

Figure 2-13.6. ***The detector response function, R(d), is plotted versus particle size for detectors S-2 (light-scattering) and R-2 (ionization).***

$$R(d) = cd \qquad (17)$$

where c has a value of 7 in units of μV per particle concentration per μm (μV $cm^3/\mu m$). Such detectors tend to be most sensitive to high concentrations of small particles, such as those produced by flaming paper and wood fires, and least sensitive to the low concentration of large smoke droplets produced in smoldering fires.

Light-scattering smoke detectors have a high sensitivity to smoke particles with diameters approximately equal to λ, the wavelength of light, and low sensitivity to

particles much smaller than λ. The response function, $R(d)$, depends on the wavelength of the light source in the smoke detector, the scattering angle, and the scattering volume. For smoke particles with diameter greater than about **0.3** μm, the output of several light-scattering smoke detectors was found to be approximately proportional to the mass concentration of the smoke.[25] Light-scattering detectors complement ionization detectors in that they have high sensitivity to smoldering fires and low sensitivity to low-smoking flaming fires, such as paper and wood fires.

The purpose of smoke detectors is to give the occupants of a room adequate warning to escape a developing fire. The final examples of this chapter illustrate how to utilize all the concepts discussed above to estimate escape time.

EXAMPLE 4:

Suppose the pillow in the preceding example is burning at a steady rate of 50 g/min. How long would it take for an ionization detector with response function given by Equation 17 to alarm? Assume an alarm voltage of 2.5 V above background. How much time would an individual have before the visibility decreased to an unsafe level?

SOLUTION:

First consider a first principle analysis based on the size distribution of the smoke. From Equations 16 and 17,

$$P = c\int_{d_{\min}}^{d_{\max}} d\,\frac{\delta N}{\delta d}\,\delta d$$

The following three identities[9] for the log-normal distribution are needed:

$$\int_0^\infty d\,\frac{\delta N}{\delta d}\,\delta d = N_0 d_{gn}\exp\left(\frac{1}{2}\ln^2\sigma_g\right) \qquad \text{(I-1)}$$

$$\int_0^\infty d^3\,\frac{\delta N}{\delta d}\,\delta d = N_0 d_{gn}^3\exp\left(\frac{9}{2}\ln^2\sigma_g\right) \qquad \text{(I-2)}$$

Here N_0 refers to the number concentration. Taking $(\delta N/\delta d)$ to be log-normal and using Equation I-1,

$$P = cN_0 d_{gn}\exp\left(\frac{1}{2}\ln^2\sigma_g\right)$$

Estimating σ_g to be 2.0, d_{gn} to be 0.1 μm for flexible polyurethane, and c to be 7 μV·cm³/μm, the following expression is obtained for P:

$$P = cN_0\left(d_{gn}\right)\exp\left(\frac{1}{2}\ln\sigma_g^2\right) = 7N_0(0.10)\exp\left[\frac{1}{2}(0.69)^2\right]$$

$$P = 0.89N_0\ \mu\text{m/cm}^3$$

The final task is to estimate N_0 based on the mass generation rate of smoke. In one minute, 50 g of the pillow are consumed and 1.5 g of smoke are produced. This corresponds to a mass concentration, m, given by

$$m = \frac{1.5}{(6)^2(2.5)} = 0.0167\ \text{g/m}^3 = 1.67\times10^{-8}\ \text{g/cm}^3$$

The quantity m is the third moment of the size distribution,

$$m = \int_0^\infty \frac{1}{6}\pi\rho d^3\,\frac{\delta N}{\delta d}\,\delta d$$

Using Equation I-2,

$$m = \frac{1}{6}\pi\rho N_0 d_{gn}^3\exp\left(\frac{9}{2}\ln^2\sigma_g\right)$$

Finally, solving for N_0,

$$N_0 = \frac{6m}{\pi\rho d_{gn}^3}\exp\left(-\frac{9}{2}\ln^2\sigma_g\right)$$

$$= \frac{(6)(1.67\times10^{-8})}{(3.14)(2)(1.0\times10^{-5})^3}\exp\left[-\frac{9}{2}\ln^2(2.0)\right]$$

$$N_0 = 1.8\times10^6\ \text{particles/cm}^3\ (\text{assuming}\ \rho = 2\ \text{g/cm}^3)$$

Substituting in the expression for P,

$$P = (0.89)(1.8\times10^6) = 1.6\times10^6\ \mu\text{V} = 1.6\ \text{volts}$$

This represents the voltage after 1 min. The estimated time to reach the alarm point, 2.5 V, will be 1.6 min. By the time the entire pillow is consumed in 4 min, the visibility has deteriorated to the point where escape is becoming less likely (visibility 5.9 m, according to Example **3**, for a room 6 m across). So the individual's escape time is as follows:

escape time = time to unsafe condition minus time to detector alarm

= **4** – 1.6 = 2.4 min

Example 4 is intended to illustrate the complete method for estimating the alarm time of smoke detectors. However, there is not adequate information at this time to implement the method in a realistic manner. Information on the size distribution and on the detector response functions is lacking for smoke agglomerates. The time for the smoke to reach the detector and the time lag for the smoke to enter the sensing zone of the detector are not included in this example, but should be included in a full analysis of the problem.

A simpler method for estimating the alarm time is to calculate the time at which the optical density per meter of the smoke exceeds the value of 0.06 (gray smoke) or 0.14 (black smoke), which correspond to the U.L. minimum sensitivity values. The limitation of this procedure is that a detector set to alarm at a particular optical density for one type of smoke may not respond in the same manner to another with a different size distribution and refractive index.

EXAMPLE 5:

Estimate the alarm time for the conditions given in Example 4, using the simpler method described above.

SOLUTION:

In Example 3, the optical density was estimated to be 0.49 m⁻¹, based on D_m measured for polyurethane. This

value corresponds to the burning of the entire pillow. Assuming a steady smoke generation rate, the alarm time [the time at which the minimum detector sensitivity value is exceeded (0.14 for black smoke)] is estimated to be given by

$$t = \frac{0.14}{0.49}(4) = 1.1 \text{ minutes}$$

This is comparable to the estimated 1.6 minutes in Example 4.

Nomenclature

ε	smoke conversion factor
d	particle diameter (pm)
d_i	midpoint of the ith particle size channel (pm)
d_{gn}	geometric mean number diameter (μm)
d_{gv}	geometric mean volume diameter (μm)
d_{32}	volume surface mean diameter (pm)
σ_g	geometric standard deviation
N	number concentration (particles/cm³)
m	mass concentration of smoke (mg/m³ or g/m³)
V_T	volume concentration of smoke (cm³/m³ or μm³/cm³)
$\frac{\Delta N}{\Delta d}$ or $\frac{dN}{dd}$	number size distribution function cm⁻³·μm⁻¹
$\frac{\Delta N}{\Delta \log d}$ or $\frac{dN}{d \log d}$	geometric number size distribution function (cm⁻³)
$\frac{\Delta m}{\Delta d}$ or $\frac{dm}{dd}$	mass size distribution function (mg·μm⁻¹·m⁻³)
Q_{ext}	extinction efficiency
λ	wavelength of light (pm)
n_r	complex refractive index of smoke particles
K	extinction coefficient (m⁻¹)
D	optical density per meter (m⁻¹)
K_m	specific extinction coefficient (m²/g)
D_s	specific optical density
D_m	mass optical density (m²/g)
I_λ	intensity of light at wavelength λ
B	luminance
C	contrast
s	visibility range (m)
L	pathlength
Γ	coagulation coefficient (cm³/s)
t	time
ΔM	mass loss of sample (g)
P	detector output (V)
$R(d)$	detector size response function (pv cm³)
V_c	volume of chamber (m3)
A	area of sample (m²)
M_s	mass of smoke (g)

References Cited

1. C.P. Bankston, B.T. Zinn, R.F. Browner, and E.A. Powell, *Comb. and Flame*, 41, p. 273 (1981).
2. C.J. Hilado and A.M. Machado, *J. Fire and Flamm.*, 9, p. 240 (1978).
3. C.P. Bankston, R.A. Cassanova, E.A. Powell, and B.T. Zinn, *NBS-GCR* G8-9000, National Bureau of Standards, Washington, DC (1978).
4. S.K. Brauman, N. Fishman, A.S. Brolly, and D.L. Chamberlain, *J. Fire and Flamm.*, 6, p. 41 (1976).
5. A. Tewarson, J.L. Lee, and R.F. Pion, *18th Symposium (International) on Combustion*, Pittsburgh, PA (1981).
6. G.W. Mulholland and T.J. Ohlemiller, *Aerosol Sci. and Tech.*, **1**, p. 59 (1982).
7. G.W. Mulholland, T.G. Lee, and H.R. Baum, *J. Colloid Interface Sci.*, 62, p. 406 (1977).
8. S.K. Friedlander, *Smoke, Dust and Haze*, John Wiley and Sons, New York (1977).
9. P.C. Reist, *Introduction to Aerosol Science*, Macmillan, New York (1984).
10. T. Waldman and K.H. Schmitt, in *Aerosol Science*, Academic Press, New York (1966).
11. J.D. Seader and I.N. Einhorn, *16th Symposium (International) on Combustion*, Combustion Institute, Pittsburgh, PA (1976).
12. W.W. Foster, *Br. J. App. Phys.*, 10, p. 416 (1959).
13. G.W. Mulholland, *Fire and Matls.*, 6, p. 65 (1982).
14. D. Gross, J.J. Loftus, and A.F. Robertson, *ASTM STP* 422, American Society for Testing and Materials, West Conshohocken, PA (1967).
15. J.D. Seader and W.P. Chien, *J. Fire and Flamm.*, 5, p. 151 (1974).
16. L.H. Breden and M. Meisters, *J. Fire and Flamm.*, 7, p. 234 (1976).
17. E.L. Lopez, *J. Fire and Flamm.*, 6, p. 405 (1975).
18. V. Babrauskas, *J. Fire and Flamm.*, 12, p. 51 (1981).
19. D.D. Evans, *NBSIR 81-2400*, National Bureau of Standards, Washington, DC (1981).
20. J.G. Quintiere, *Fire and Matls.*, 6, p. 145 (1982).
21. E.J. McCartney, *Optics of the Atmosphere*, Wiley and Sons, New York (1976).
22. T. Jin, *J. Fire and Flamm.*, 9, p. 135 (1978).
23. T. Jin and T. Yamada, *Fire Sci. and Tech.*, 5, p. 79 (1985).
24. UL 217, *Standard for Single and Multiple Station Smoke Detectors*, Underwriters Laboratories, Northbrook, IL (1993).
25. G.W. Mulholland and B.Y.H. Liu, *J. Res. NBS*, 85, p. 223 (1979).
26. C. Helsper, H. Fissan, J. Muggli, and A. Scheidweiler, *Fire Tech.*, 14 (1983).